

Thouless Energy and Correlations of QCD Dirac Eigenvalues

J.C. Osborn and J.J.M. Verbaarschot

Department of Physics and Astronomy, SUNY, Stony Brook, New York 11794

Abstract

Eigenvalues and eigenfunctions of the QCD Dirac operator are studied for gauge field configurations given by a liquid of instantons. We find that for energy differences δE below an energy scale E_c the eigenvalue correlations are given by Random Matrix Theories with the chiral symmetries of the QCD partition function. For eigenvalues near zero this energy scale shows a weak volume dependence that is not consistent with $E_c \sim 1/L^2$ which might be expected from the pion Compton wavelength and from the behavior of the Thouless energy in mesoscopic systems. However, the numerical value of E_c for our largest volumes is in rough agreement with estimates from the pion Compton wavelength. A scaling behaviour consistent with $E_c \sim 1/L^2$ is found in the bulk of the spectrum. For $\delta E > E_c$ the number variance shows a linear dependence with a slope which is larger than the nonzero multifractality index of the wave functions. Finally, the average spectral density and the scalar susceptibilities are discussed in the context of quenched chiral perturbation theory. We argue that a nonzero value of the disconnected scalar susceptibility requires a linear dependence of the number variance on δE .

1 Introduction

Random matrix theories have been applied extensively to disordered mesoscopic systems (for recent reviews we refer to [1, 2, 3]). In particular, correlations of energy eigenvalues have been studied in great detail. One important energy scale that enters in these studies is the Thouless energy, E_c , which is essentially the inverse diffusion time of an electron through the sample [4]. If the diffusion constant is given by D and the linear dimension of the sample is equal to L the Thouless energy is given by

$$E_c = \frac{\hbar D}{L^2}. \quad (1)$$

What has been found is that eigenvalues closer than E_c are correlated according to the invariant random matrix ensembles. Because such correlations are characteristic for classically ergodic and chaotic quantum system this regime is also known as the ergodic energy domain. A second energy scale is given by \hbar/τ_e , where τ_e is the elastic collision time. The energy regime with $\delta E > \hbar/\tau_e$ is known as the ballistic regime whereas the domain $E_c < \delta E < \hbar/\tau_e$ is known under the names of diffusive regime or Altshuler-Shklovskii regime. The different energy regimes have received a great deal of attention in recent literature [5, 6, 7, 8, 9, 10, 11] (for further references we refer to [1, 2, 3]). A semiclassical interpretation in terms of the return probability has been given in [12].

A convenient way to measure the pair correlations of eigenvalues is by means of the number variance $\Sigma_2(n)$. This statistic is defined as the variance of the number of eigenvalues in an interval containing n eigenvalues on average. In the ergodic regime the number variance is given by the invariant random matrix ensembles $\Sigma_2(n) \sim (2/\beta\pi^2) \log(n)$. The behavior of the number variance in the diffusive is less well-established. One proposal is [4] that $\Sigma_2(n) \sim n^{d/2}$ (where d is the number of Euclidean dimensions) if the coupling is below the critical value for a localization transition. However, for critical values of the coupling constant, for which the localization length scales with the size of the sample, a linear dependence on n is predicted, i.e., $\Sigma_2(n) \sim \chi n$. In this regime, the slope has been related to the multifractality index of the wave functions [13, 14].

In this letter we investigate to what extent such scenarios are realized in QCD. In QCD the order parameter of the chiral phase transition is related to the spectral density,

$\rho(\lambda)$, of the Dirac operator by means of the Banks-Casher formula [15], $\Sigma = \lim \pi\rho(0)/V$ (the space-time volume is denoted by $V = L^4$). For broken chiral symmetry, $\Sigma \neq 0$, this results in eigenvalues near zero virtuality that are spaced as $\sim 1/V$. It is therefore natural to introduce the microscopic limit $V \rightarrow \infty$ such that $u = \lambda V \Sigma$ is kept constant. The microscopic spectral density is then defined by [16],

$$\rho_S(u) = \lim_{V \rightarrow \infty} \frac{1}{V\Sigma} \langle \rho(\frac{u}{V\Sigma}) \rangle, \quad (2)$$

where the spectral density is defined by

$$\rho(\lambda) = \sum_k \delta(\lambda - \lambda_k), \quad (3)$$

and the brackets denote ensemble averaging. There is ample evidence from lattice QCD [17, 18, 19] and instanton liquid simulations [20] that $\rho_S(u)$ and other correlators on the scale of individual level spacings [21] are given by chiral Random Matrix Theory, i.e. random matrix theories with the chiral symmetries of the QCD partition function. However, at scales beyond a few eigenvalue spacings in both instanton simulations [20] and lattice QCD simulations [17, 18] the Dirac eigenvalues near zero show stronger fluctuations than those in the chiral random matrix theories. This indicates the presence of an energy scale in QCD which may be identified as the Thouless energy.

In the regime where the pion loops can be ignored the correlations of the eigenvalues near zero are given by the chiral random matrix ensembles [16, 22]. They can be mapped onto an effective partition function given by the mass term generated by the spontaneous breaking of chiral symmetry [16]. From the work of Gasser, Leutwyler and Smilga [23, 24], we expect that the boundary of the ergodic regime is given by a mass scale m_c where the Compton wavelength of the associated Goldstone boson with mass $m_\pi^2 = m_c K$ (according to the PCAC relation $K = \Sigma/F_\pi^2$, where F_π is the pion decay constant) is of the order of the linear dimension of the box. This condition can be written as [25, 26]

$$m_c = \frac{1}{KL^2}. \quad (4)$$

It is therefore tempting to interpret $1/K$ as the diffusion constant. Because K is large on a hadronic scale ($K \approx 1660 \text{ MeV}$) the diffusion constant is relatively small, and we expect a Thouless energy that is small as well. We emphasize that m_c is a valence quark

mass that is not present in the fermion determinant. In other words, the spectral density does not depend on m_c . For example, the valence quark mass of the chiral condensate is related to the spectral density by [27]

$$\Sigma(m) = \frac{1}{V} \int_0^\infty \frac{2m\rho(\lambda)d\lambda}{\lambda^2 + m^2}. \quad (5)$$

Therefore, the spectral density and, similarly, higher order correlation functions, can be obtained from the valence quark mass dependence of the effective partition function. It can be obtained with the help of quenched chiral perturbation theory [28] or by means of the replica trick in which we start from n_f valence flavors and take the limit $n_f \rightarrow 0$ at the end of the calculation. In the thermodynamic limit, the mass scale (4) is much less than the scale of massive quarks which leads to a decoupling of the valence quark mass dependent part of the partition function. The Dirac spectrum and its correlations are thus given by the valence quark mass dependence of the effective partition function which below the scale (4) is given by chiral random matrix theory. For massless quarks the argument is simpler. Now the Compton wavelength of the physical pions is always much larger than the size of the box. The crossover point is thus given by the value of the valence quark mass where the corresponding Goldstone boson (in the sense of quenched or partially quenched chiral perturbation theory) is equal to the size of the box. In this case, however, the microscopic spectral correlations depend on the number of massless flavors. Alternatively, one can study the boundaries of the domain where the pion loops can be neglected via relations between microscopic spectral correlators and finite volume partition functions as given in [29].

In the bulk of the spectrum, chiral symmetry is broken explicitly by the valence quark mass, and the 'Goldstone bosons' associated with the valence quark masses are no longer in the low energy spectrum of QCD. However, in this case, spontaneous symmetry breaking in the generating function for the correlation functions results in the usual nonlinear σ -model for disordered mesoscopic systems [30]. The critical energy scale is then given by the Thouless energy $m_c \sim 1/K'L^2$, where $K' = \pi\rho(E)/VF_\pi^2$ and $\rho(E)$ is the spectral density at E . Since the group manifold is different in this case [31] the numerical constant in this relation differs by a factor of the order unity from the constant in (4).

Using that according to the Banks Casher relation [15] the eigenvalue spacing is given

by $\Delta = \pi/\Sigma V$, the condition (4) can be rewritten in dimensionless form as

$$g_c = \frac{m_c}{\Delta} = \frac{F_\pi^2}{\pi} L^2. \quad (6)$$

Here, g_c plays the role of the dimensionless conductivity. At this point we wish to mention that a relation between transport properties of mesoscopic systems and the pion decay constant was established recently in [32]. In lattice QCD for an Na^4 lattice this relation reads $g_c = F_\pi^2 a^2 \sqrt{N}/\pi$. On a 16^4 lattice with a lattice spacing of $0.1 fm$ this results in a dimensionless Thouless energy of a couple of lattice spacings.

In order to investigate the presence of a Thouless energy in QCD we perform our calculations for gauge field configurations given by a liquid of instantons. For such configurations we study correlations of the eigenvalues of the corresponding Dirac operator. In particular, we investigate the number variance, and establish a crossover between the ergodic and the diffusive domain. The linear dependence will be compared with the multifractality index of the wave functions. We will argue that results for chiral perturbation theory apply to the diffusive regime. The above observables are studied for a variety of system sizes and as a function of the number of flavors.

2 Instanton liquid model

In this model the gauge field configurations are given by a superposition of instantons. We use the streamline Ansatz which for a dilute system reduces to the sum Ansatz defined as a simple superposition of instanton profiles $A_\mu = \sum_I A_{I,\mu}$. Each instanton is described by $4N_c$ (the number of colors is denoted by N_c) collective coordinates. The Euclidean QCD partition function is then approximated by

$$Z_{\text{inst}} = \int D\Omega \det^{N_f}(\gamma \cdot D + m) e^{-S_{\text{YM}}}, \quad (7)$$

where the integral is over the collective coordinates of the instantons and the covariant derivative is defined by $D_\mu = \partial_\mu + iA_\mu$. The Yang-Mills action of the gauge field configurations is denoted by S_{YM} . We will only consider configurations with an equal number of instantons and anti-instantons. The fermion determinant is evaluated in the space of the fermionic zero modes of the instantons.

This partition function obeys the flavor and chiral symmetries of the QCD partition function. It reproduces results obtained in chiral perturbation theory as well as many other details of the low energy hadronic phenomenology [33, 34, 35, 36]. In our calculations we use the standard instanton liquid parameters with instanton density $N/V = 1$ (in units of fm^{-1}). For more details on the instanton liquid partition function we refer to a recent review by Schäfer and Shuryak [37].

3 Random matrix model

The chiral random matrix ensembles for N_f massless quarks in the sector of topological charge ν are defined by the partition function [16, 22]

$$Z_{N_f, \nu}^\beta = \int DW \det^{N_f} \begin{pmatrix} 0 & iW \\ iW^\dagger & 0 \end{pmatrix} e^{-n\beta \text{Tr} V(W^\dagger W)}, \quad (8)$$

where W is a $n \times (n + \nu)$ matrix. As is the case in QCD, we assume that ν does not exceed $\sqrt{2n}$. The parameter $2n$ is identified as the dimensionless volume of space time. It can be thought of as the total number of instantons in the partition function (7). The matrix elements of W are either real ($\beta = 1$, chiral Orthogonal Ensemble (chOE)), complex ($\beta = 2$, chiral Unitary Ensemble (chUE)), or quaternion real ($\beta = 4$, chiral Symplectic Ensemble (chSE)). The simplest ensemble is the Gaussian case with $V(x) = \Sigma^2 x$ (also known as the Laguerre ensemble). In that case one can easily show that the microscopic spectral density (2) is given by [22]

$$\rho_S(u) = \frac{u}{2} (J_a^2(u) - J_{a+1}(u)J_{a-1}(u)). \quad (9)$$

where $a = N_f + |\nu|$ (the result for $a = 0$ was obtained in [38]). It is also straightforward to derive the microscopic correlation functions [38, 18]. In the bulk of the spectrum, the eigenvalue correlations of the chiral ensembles are given by the invariant random matrix ensembles.

It was shown by Akemann et al. [39] that, for $\beta = 2$, the microscopic spectral density and the microscopic spectral correlators do not depend on the potential $V(x)$ and are given by the results [38] for the Laguerre ensemble. Their work greatly extends an earlier result by Brézin and Zee [40] who studied the potential $V(x) = x + \alpha x^2$. The microscopic spectral density is also invariant with respect to the addition of an arbitrary constant

matrix to the off-diagonal blocks in the determinant [41, 42]. The application of chRMT has been put on a firm foundation by these and other universality proofs [43]. Whether or not QCD is in this universality class is a dynamical question that only can be proven by explicit numerical simulations.

4 Numerical Results

In this section we simulate the instanton liquid model introduced in section 2. We evaluate the partition function (7) by means of a Metropolis algorithm. Typically, we perform on the order of 10,000 sweeps for each set of parameters. For the equilibrated configurations the eigenvalues and eigenvectors of the Dirac operator are calculated by means of standard diagonalization procedures. Most of our calculations have been performed in the quenched approximation ($N_f = 0$). The motivation for this choice is twofold. First, calculations at $N_f \neq 0$ require the evaluation of a determinant for each update of the integration variables which is extremely costly and restricts us to a total number of instantons not larger than 128. For $N_f = 0$, we are able to generate ensembles up to 512 instantons which turns out to be important in the study of the thermodynamic limit. Second, our results are compared with ideas from disordered mesoscopic systems where no fermion determinant is present.

In order to separate the fluctuations of the eigenvalues from the average spectral density we unfold the spectrum, i.e. we rescale the spectrum in units of the local average level spacing. Specifically, the unfolded spectrum λ_k^{unf} is obtained from the original spectrum λ_k according to

$$\lambda_k^{\text{unf}} = \int_0^{\lambda_k} \bar{\rho}(s) ds, \quad (10)$$

where $\bar{\rho}(s)$ is the smoothed average spectral density. The number variance, the nearest neighbor spacing distribution and the microscopic spectral density are all calculated from the unfolded spectrum.

In Figs. 1 and 2 we show the number variance, $\Sigma_2(n)$ versus n for $N_f = 0$ and various total numbers of instantons as given in the legend of the figure. The instanton density $N/V = 1$. The random matrix result for $\Sigma_2(n)$ for the chGUE [18] is depicted by the

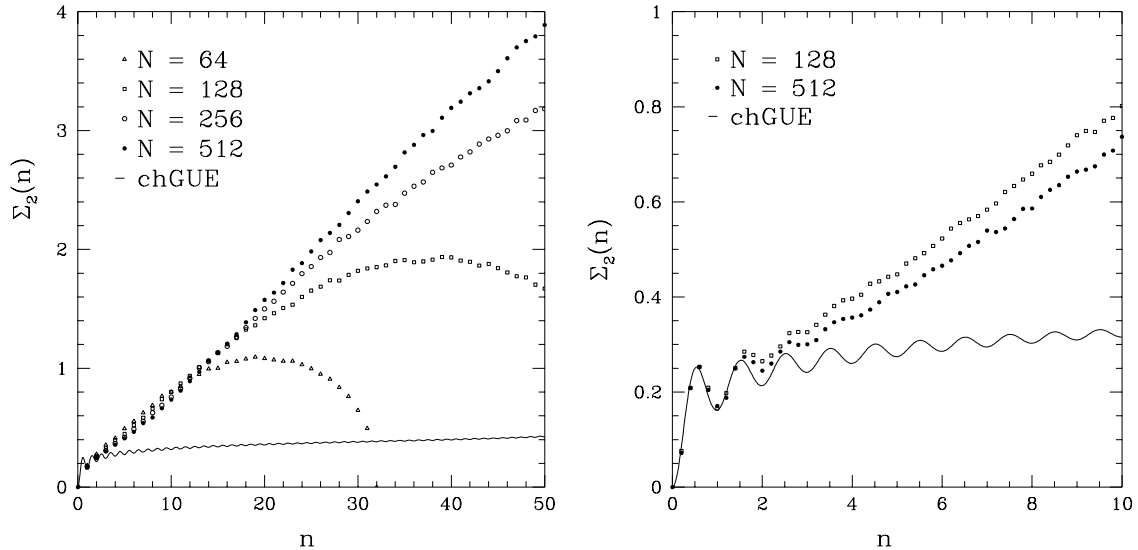


Fig. 1. The number variance $\Sigma_2(n)$ versus n in the quenched approximation for an interval starting at $\lambda = 0$. The total number of instantons is indicated in the legend of the figure.

solid curve. In both figures, the right figure (with results for only two different volumes) is a blown-up version of the left figure. In Fig. 1 the number variance is calculated for the interval that contains on average the n smallest positive eigenvalues. Fig. 2 represents the number variance in the bulk of the spectrum obtained from an interval that is symmetric about the average unfolded positive eigenvalue. In both cases we observe a transition point n_c below which the number variance is given by random matrix theory. In Fig. 1 the value of the crossover point, $n_c \approx 2$, depends only weakly on the total number of instantons (or the volume). This is not in agreement with the theoretical expectation (6) that $n_c \approx F_\pi^2 \sqrt{V} / \pi$ in four dimensions. For standard instanton liquid parameters the numerical value of n_c for N instantons is given by $n_c \approx 0.08 \sqrt{N}$ which is on the order of the results found in Fig. 1. In the bulk of the spectrum (Fig. 2) the value of n_c is consistent with a \sqrt{V} scaling but the numerical constant appears to be larger than the above estimate (even if we take into account that the spectral density in the bulk is considerably less than near $\lambda = 0$). This result is in agreement with the finding that correlations of lattice QCD eigenvalues for 12^4 and 16^4 lattices are given by RMT up to distances of 100 and 300 level spacings, respectively [21, 44]. Notice that the condition that the pion Compton wavelength is equal to the size of the box (leading to (4)) provides us only with an order of magnitude estimate for the transition point.

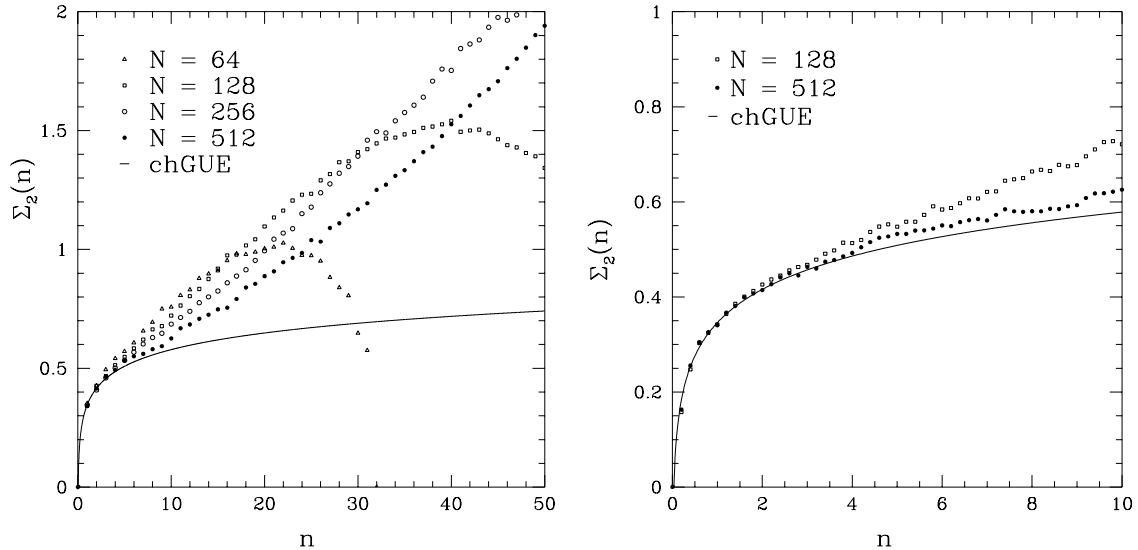


Fig. 2. The number variance $\Sigma_2(n)$ versus n in the bulk of the spectrum in the quenched approximation and a total number of instantons as indicated in the legend of the figure.

Beyond the crossover point the number variance shows a linear behavior with a slope $\chi \approx 0.08$ for eigenvalues near zero and $\chi \approx 0.04$ in the bulk of the spectrum. The downward trend of the curves for larger values of n is a finite size effect. For example, for a finite number of uncorrelated eigenvalues $\Sigma_2(n)$ does not behave linearly, but rather as $\Sigma_2(n) = n - 2n^2/N$ (notice that we have only $N/2$ positive eigenvalues). This finite size effect prevents us from saying more about the ballistic regime, an energy scale of roughly the inverse distance between instantons.

In the ergodic regime we expect that eigenvalue correlations are given by the invariant random matrix ensembles. This is shown in Fig. 3 where we plot the nearest neighbor spacing distribution $P(S)$ versus S (left) and the microscopic spectral density $\rho_S(z)$ versus z (right) (in terms of the variable $z = u/\pi$ in (2)). The full circles and the open squares represent results for 512 and 128 instantons, respectively. Results obtained for the (chiral) random matrix ensembles are depicted by the full line. Clearly, below the Thouless energy we are in close agreement with RMT. However, beyond the Thouless energy of about two level spacings the oscillatory structure in the microscopic spectral density is no longer reproduced. This implies that beyond this point the QCD Dirac eigenvalues fluctuate more than the chGUE eigenvalues which is consistent with the number variance shown

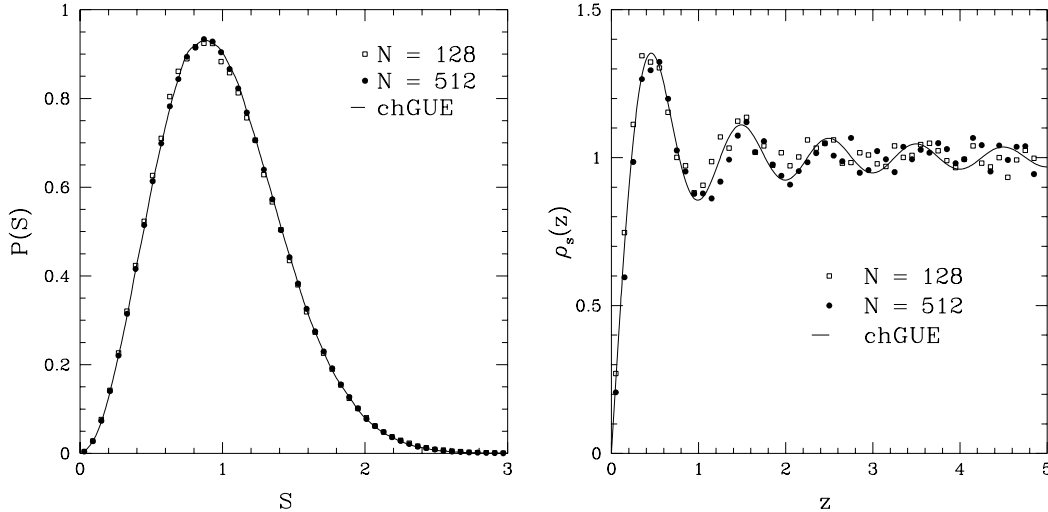


Fig. 3. The nearest neighbor spacing distribution $P(S)$ versus S (left) and the microscopic spectral density $\rho_S(z)$ versus z (right). The full circles and the open squares represent results for 512 and 128 instantons, respectively. Results obtained from the (chiral) random matrix ensembles are depicted by the full line.

in Fig. 1. A similar increase in eigenvalue fluctuations at a scale of a few eigenvalue spacings has been observed in lattice QCD spectra [17] indicating that also in that case the Thouless energy for the region around $\lambda = 0$ is less than predicted by the scaling behavior of disordered mesoscopic systems.

The inverse participation ratio which is a measure for the number of significant components in the wave function is defined as

$$I_2(\lambda) = \left\langle \sum_k |\psi_k(\lambda)|^4 \right\rangle, \quad (11)$$

The $\psi_k(\lambda)$ are the normalized eigenfunctions of the Dirac operator in the space of fermionic zero modes corresponding to eigenvalue λ . The number of components of the wave function will be denoted by N . For the chGUE we find $I_2 = 2/(N+2)$ whereas for uncorrelated eigenvalues (the chiral Poisson ensemble) we find $I_2 = 1/2$. Results for $NI_2(\lambda)$ as a function of λ are depicted in Fig. 4 (left). The general impression is that the wave-functions are extended with a participation ratio that is not too different from the random matrix result (full line). The eigenfunctions corresponding to small and large eigenvalues appear to be somewhat more localized. A more definitive result for the character of the wavefunctions follows from the scaling behavior of $I_2(\lambda)$ with the volume.

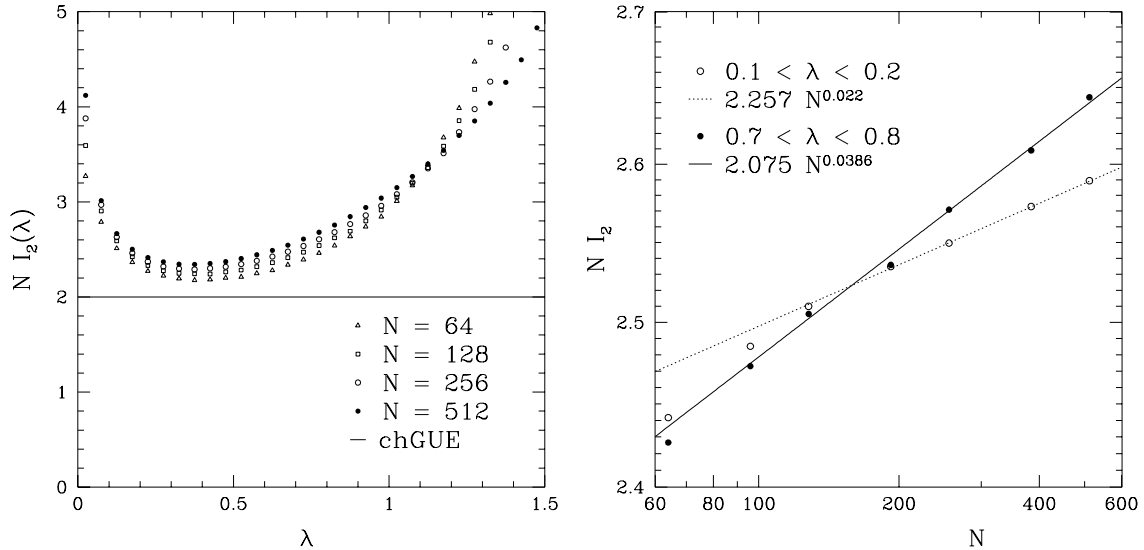


Fig. 4. The inverse participation ratio times N versus the corresponding Dirac eigenvalues for $N_f = 0$ (left) and a total number of instantons equal to 64, 128, 256 and 512, and the scaling behavior versus N (right) for the energy intervals $[0.1, 0.2]$ and $[0.7, 0.8]$.

A double logarithmic plot of $N I_2(\lambda)$ versus N is shown in Fig. 4 (right). Results are given both for the energy intervals $[0.1, 0.2]$ (open circles) and $[0.7, 0.8]$ (full circles). The first region corresponds to a part of the spectrum where the number variance shows a linear behavior for the volumes shown in Fig. 1, and the second region corresponds to the bulk of the spectrum.

The multifractality index η of the wave functions is defined by [13]

$$I_2 \sim V^{\eta/d-1}. \quad (12)$$

According to an argument given in [13] the value of $\eta = 2\chi d$ (where χ is the slope of the linear piece in the number variance) in the critical domain. From the volume dependence of the inverse participation ratio shown in Fig. 4 (right) we find a value for η/d of about 0.02 and 0.04 for the intervals $[0.1, 0.2]$ and $[0.7, 0.8]$, respectively. These values are well below the theoretical result of 2χ . Apparently, the ensemble of instantons is not in the critical region for $N_f = 0$. The localization properties of eigenfunctions have also been studied for the Wilson lattice QCD Dirac operator [45]. In that case it was found that the eigenstates are localized. We have no explanation for this discrepancy.

The flavor dependence of the number variance of eigenvalues near zero is shown in Fig. 5. Results are given for 128 instantons and massless flavors. Again the Thouless energy

is about two level spacings (in order to avoid a cluttered figure we have not plotted the random matrix results for the number variance). We observe an enhancement of eigenvalue fluctuations for 3 flavors (chiral symmetry is already restored for $N_f = 4$ [37]) and conclude that the critical number of flavors is approximately equal to three. However, our volumes (of up to 128 instantons) were too small to reliably extract the multifractality index. For completeness we mention that a similar enhancement of fluctuations for $N_f = 3$ also takes place in the bulk of the spectrum.

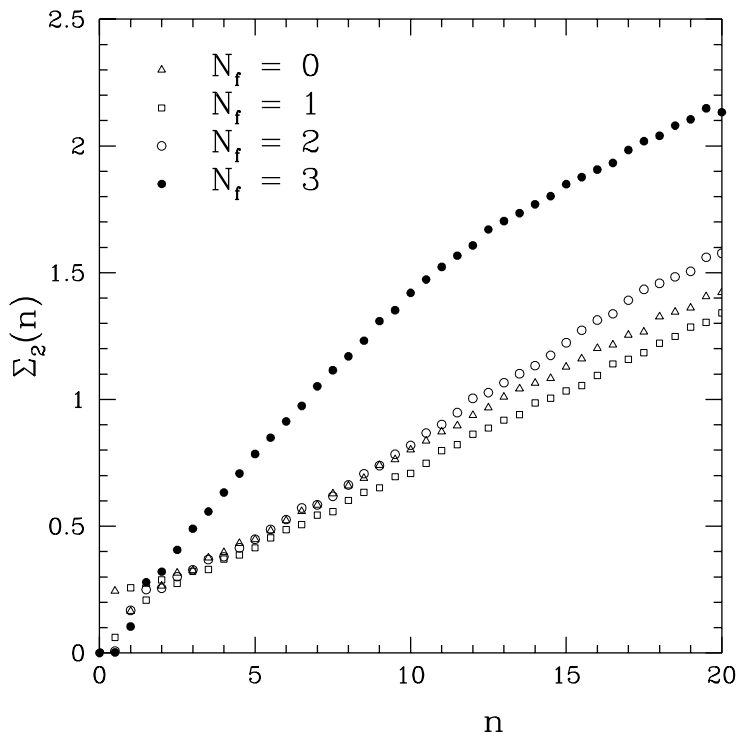


Fig. 5. The flavor dependence of the number variance $\Sigma_2(n)$ versus n calculated for an ensemble of 128 instantons.

5 Spectral density and chiral susceptibility

In this section we consider the average spectral density, the valence quark mass dependence of the chiral condensate and the connected and disconnected scalar susceptibilities. In order to compare our results with quenched chiral perturbation theory [28] we put particular emphasis on the extrapolation to the thermodynamic limit. These quantities were calculated elsewhere for smaller volumes (64 instantons) [26, 46].

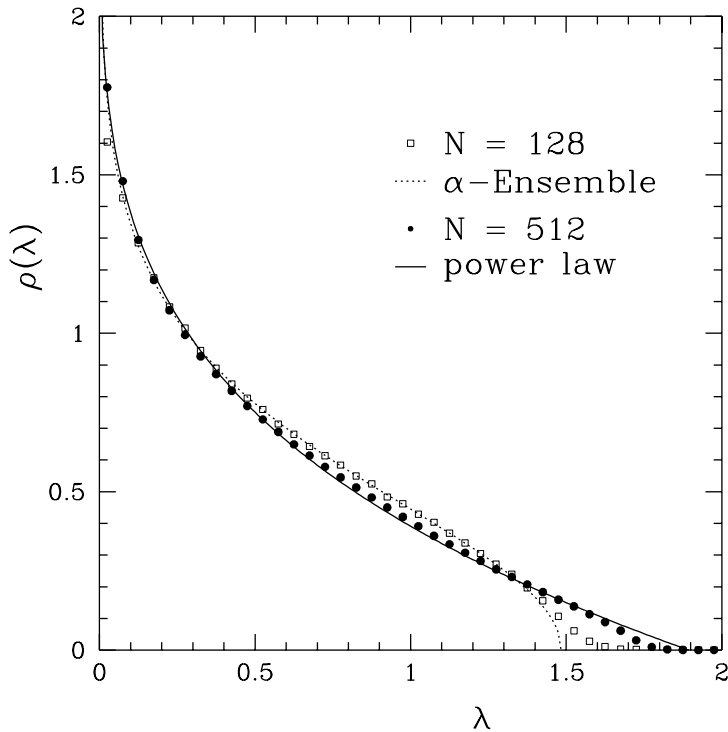


Fig. 6. The normalized spectral density $\rho(\lambda)$ versus λ for $N_f = 0$ and 128 and 512 instantons.

The spectral density of the Dirac eigenvalues for a liquid of instantons was studied before for $N_f = 0$ with the help of mean field techniques [34, 33]. For large values of N_c the overlap matrix elements are independent resulting in a semi-circular distribution [34]. For small values of N_c the matrix elements are correlated and the natural distribution is a Gaussian [33]. On the other hand, from the asymptotic dependence of the matrix elements of the Dirac operator it was concluded that [47] the spectral density diverges as $1/\sqrt{\lambda}$. Another estimate comes from quenched chiral perturbation theory [28]. For $\lambda \rightarrow 0$ one obtains a linear dependence [48] for $N_f \neq 0$, and a logarithmic divergence [49] for $N_f = 0$. For $N_f \neq 0$ the slope of the Dirac spectral density for $\lambda \rightarrow 0$ is consistent with the analytical result [50]. Here we only consider the quenched case.

In order to study the thermodynamic limit of the spectral density we have unfolded the calculated spectrum with the known result for the microscopic spectral density. The resulting normalized average spectral density for $N_f = 0$ is shown in Fig. 6. Inspection of the normalized eigenvalue density in an interval $[0.0, 0.05]$ shows that it grows logarithmically with N . This suggests that $\rho(\lambda)$ diverges for $\lambda \rightarrow 0$ in the thermodynamic limit. In

order to understand the nature of this divergence we have compared results obtained for the instanton liquid with the analytical results for the a chiral version of the α -ensembles [51] (dotted curve). These are random matrix ensembles with potential $V(x) = x^{\alpha/2}$ in (8). The spectral density of the chiral α -ensembles diverges logarithmically for $\lambda \rightarrow 0$ at $\alpha = 1$. The value of $\rho(0)$ is finite for $\alpha > 1$. For $N = 64, 128, 256$ and 512 we find $\alpha = 1.217, 1.132, 1.073, 1.039$ by fitting to the energy interval $[0.05, 0.5]$, respectively. In the thermodynamic limit this extrapolates to a value of $\alpha = 1.00 \pm 0.02$, resulting in a logarithmic divergence of the spectral density. We also compare the average spectral density to a simple power law behavior $a - b\lambda^\beta$. We find that the spectra are equally well fitted by such dependence (see full curve in Fig. 6). By fitting to the interval $[0.05, 0.5]$ we find $\beta = 0.28, 0.25, 0.13, 0.09$ for $N = 64, 128, 256,$ and 512 , respectively. This extrapolates to a value of $\beta = 0.03 \pm 0.04$ and is also consistent with a logarithmic singularity for $\lambda \rightarrow 0$. We conclude that our results are consistent with an average spectral density that diverges logarithmically for $\lambda \rightarrow 0$ in the limit $V \rightarrow \infty$. However, larger volumes need to be studied in order to arrive at definite conclusions. We wish to emphasize that our results disagree with estimates obtained by mean field methods.

The valence quark mass dependence of the chiral condensate defined in (5) is shown in Fig. 7. Results are given for $N_f = 0$ and different values of the total number of instantons. The downward trend for small masses is a finite size effect that can be understood analytically in terms of the microscopic spectral density [25]. The large volume dependence of the "plateau" prevents us from comparing our results with quenched chiral perturbation theory [28] which predicts a logarithmic dependence on the valence quark mass. For the same reason, the connected scalar susceptibility, $\partial_m \Sigma(m)$, shows an even larger volume dependence.

Finally, we consider the disconnected scalar susceptibility. It is related to the two-point correlation function according to the formula [52]

$$\chi_d = \frac{-2}{V} \int_0^\infty \int_0^\infty d\lambda d\lambda' \frac{m_1 m_2 (\lambda^2 - \lambda'^2)^2 R_c(\lambda, \lambda')}{(\lambda^2 + m_1^2)(\lambda^2 + m_2^2)(\lambda'^2 + m_1^2)(\lambda'^2 + m_2^2)} \quad (13)$$

where $R_c(\lambda, \lambda')$ is the connected two-point correlation function,

$$R_c(\lambda, \lambda') = \langle \rho(\lambda) \rho(\lambda') \rangle - \langle \rho(\lambda) \rangle \langle \rho(\lambda') \rangle. \quad (14)$$

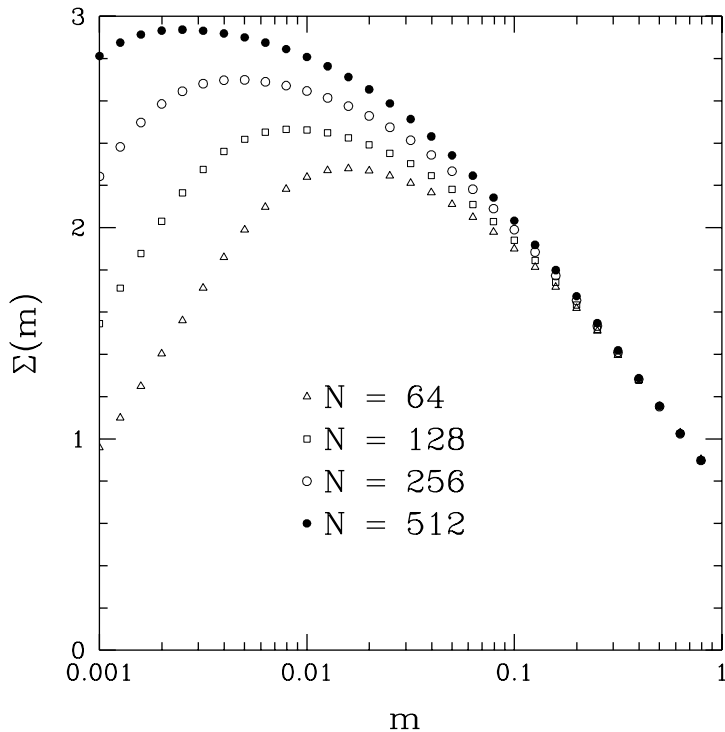


Fig. 7. The valence quark mass dependence of the chiral condensate for $N_f = 0$ and a total number of instantons as indicated in the legend of the figure.

In the derivation of (13) we have used that that R_c satisfies the sum-rule $\int_0^\infty d\lambda R_c(\lambda, \lambda') = 0$. In the bulk of the spectrum, a number variance given by $\Sigma_2(n) = \chi n$ is reproduced by a two-point correlation function $R_c(\lambda, \lambda') = \chi(\delta(\lambda - \lambda')\rho(\lambda) - 2\rho(\lambda)\rho(\lambda')/N)$ (For an extensive discussion of the relation between a linear dependence of the number variance and the sum rule for the two-point function we refer to [53]). This results in the disconnected susceptibility

$$\chi_d = \chi \left(\frac{\Sigma}{m} - \partial_m \Sigma - 2\Sigma^2 \right). \quad (15)$$

A $1/m$ behavior for the susceptibility was observed in unquenched lattice QCD simulations [54]. In Fig. 8 we show the disconnected scalar susceptibility $m\chi_d/\Sigma(m)$ versus m . We observe a 'plateau' that would indicate a $1/m$ dependence for $N = 128$, but it disappears for larger volumes. Apparently, finite size effects prevent us from making any definite conclusions.

Let us finally make a naive estimate of the disconnected susceptibility. The two-point correlation function $T_2(\lambda, \lambda')$, which is related to $R_c(\lambda, \lambda')$ by $T_2(\lambda, \lambda') = \delta(\lambda - \lambda')\rho(\lambda) -$

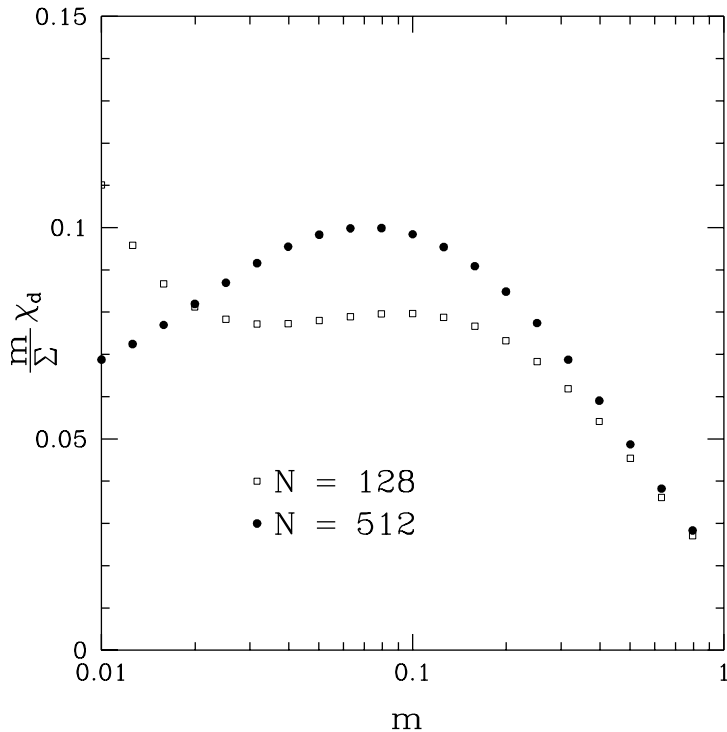


Fig. 8. The disconnected chiral susceptibility for $N_f = 0$ both for 128 and 512 instantons.

$R_c(\lambda, \lambda')$, can be expressed in terms of the two-level cluster function as

$$T_2(\lambda, \lambda') \approx \rho(\lambda)\rho(\lambda')Y_2(r), \quad (16)$$

where $r = \int_{\lambda}^{\lambda'} \rho(s)ds$. According to [9] $Y_2(r)$ is related to the number variance as

$$Y_2(r = n) = -\frac{1}{2}\partial_n^2 \Sigma_2(n). \quad (17)$$

This results in $T_2(\lambda, \lambda') \approx \frac{1}{2}\partial_{\lambda}\partial_{\lambda'}\Sigma_2(r)$. Combining (16) and (17) with (13) we find that a finite value of χ_d , which is expected according to quenched chiral perturbation theory [49] and lattice QCD simulations [54], requires that

$$\lim_{N \rightarrow \infty} \frac{\Sigma_2(Nx)}{N} \quad (18)$$

is finite. In other words, a nonzero disconnected chiral susceptibility requires a number variance that shows a linear behavior on macroscopic scales. In chiral random matrix theory we find that $\chi_d = 0$ in the thermodynamic limit. Because of the large volume dependence of the spectral density this argument could not be verified in detail. In future work, though, we hope confirm relations of this type.

6 Conclusions

We have identified an energy scale below which the eigenvalue correlations of the QCD Dirac operator are given by the chiral random matrix ensembles. In analogy with the theory of mesoscopic systems, this scale will be called the Thouless energy. For eigenvalues near zero the volume dependence of the Thouless energy is weak but its numerical value is of the same order as estimates from the pion Compton wavelength. For eigenvalues in the bulk of the spectrum the Thouless energy scales roughly with the square root of the volume which is in agreement with results from the theory of mesoscopic systems. However, we find a proportionality constant that is larger than given by our simple estimates.

For energy scales beyond the Thouless energy a linear n -dependence of the number variance is found which, according to the work by Altshuler and Shklovskii, corresponds to a critical system. We have shown that the corresponding Dirac eigenfunctions show a multifractal behavior. However, our multicritical exponents are not in agreement with relations derived for a critical system. Obviously, our ensemble of instantons is below critical. One way to increase the criticality of the system is to increase the number of flavors. However, at $N_f \neq 0$ simulations for the large volumes that are required for the extraction of the multifractality index became too costly. Alternatively, one expects that pion loops become important at energy scales beyond the Thouless energy, and that results from chiral perturbation theory apply to this region. Due to large finite size effects we were unable to make a detailed comparison. However, the spectral density near zero in the quenched approximation is consistent with a logarithmic dependence predicted by quenched chiral perturbation theory.

Acknowledgements We wish to thank A. Smilga for encouraging us to study localization properties for a liquid of instantons and Y. Fyodorov for his suggestion that the transition point in our results is related to the Thouless energy. During the completion of this work we received a preprint by R. Janik, M. Nowak, G. Papp and I. Zahed in which similar questions are discussed.

References

- [1] T. Guhr, A. Müller-Groeling and H.A. Weidenmüller, cond-mat/9707301, Phys. Rep. (in press).
- [2] C.W.J. Beenakker, Rev. Mod. Phys. **69** (1997) 731.
- [3] G. Montambaux, cond-mat/9602071.
- [4] B.L. Altshuler, I.Kh. Zharekeshev, S.A. Kotochigova and B.I. Shklovskii, Zh. Eksp. Teor. Fiz. **94** (1988) 343.
- [5] A. Altland and Y. Gefen, Phys. Rev. Lett. **71** (1993) 3339.
- [6] D. Braun and G. Montambaux, Phys. Rev. **52** (1995) 13903.
- [7] A.G. Aronov and A.D. Mirlin, Phys. Rev. **B51** (1995) 6131.
- [8] Y.V. Fyodorov and A.D. Mirlin, Phys. Rev. **B51** (1995) 13403.
- [9] T. Guhr and A. Mueller-Groeling, cond-mat/9702113, J. Math. Phys. (in press).
- [10] V.E. Kravtsov, I.V. Lerner, B.L. Altshuler and A.G. Aronov, Phys. Rev. Lett. **72** (1994) 888.
- [11] A. Altland, Y. Gefen and G. Montambaux, Phys. Rev. Lett. **76** (1996) 1130.
- [12] N. Argaman, Y. Imry and U. Smilansky, Phys. Rev. **B47** (1993) 4440.
- [13] J.T. Chalker, V.E. Kravtsov, I.V. Lerner, JETP Lett. **64** (1996) 386.
- [14] V.E. Kravtsov and I.V. Yurkevich, cond-mat/9612036.
- [15] T. Banks and A. Casher, Nucl. Phys. **B169** (1980) 103.
- [16] E.V. Shuryak and J.J.M. Verbaarschot, Nucl. Phys. **A560**, 306 (1993).
- [17] M.E. Berbenni-Bitsch, S. Meyer, A. Schäfer, J.J.M. Verbaarschot and T. Wettig, Phys. Rev. Lett. **80** (1998) 1146.
- [18] J.Z. Ma, T. Guhr and T. Wettig, hep-lat/9712026.
- [19] R. Pullirsch, K. Rabitsch, T. Wettig and H. Markum, hep-ph/9803285.
- [20] J.J.M. Verbaarschot, Nucl. Phys. **B427** (1994) 434.
- [21] M.A. Halasz and J.J.M. Verbaarschot, Phys. Rev. Lett. **74** (1995) 3920; M.A. Halasz, T. Kalkreuter and J.J.M. Verbaarschot, Nucl. Phys. Proc. Suppl. **53** (1997) 266.

- [22] J. Verbaarschot, Phys. Rev. Lett. **72** (1994) 2531; Phys. Lett. **B329** (1994) 351; Nucl. Phys. **B426**[FS] (1994) 559.
- [23] J. Gasser and H. Leutwyler, Phys. Lett. **188B**(1987) 477.
- [24] H. Leutwyler and A. Smilga, Phys. Rev. **D46** (1992) 5607.
- [25] J.J.M. Verbaarschot, Phys. Lett. **B368** (1996) 137.
- [26] J.J.M. Verbaarschot, in *Nonperturbative Approaches to Quantum Chromodynamics*, D. Diakonov, ed., Gatchina 1995.
- [27] S. Chandrasekharan, Nucl. Phys. Proc. Suppl. **42** (1995) 475; S. Chandrasekharan and N. Christ, Nucl. Phys. Proc. Suppl. **42** (1996) 527; N. Christ, Lattice 1996.
- [28] M.F.L. Golterman and K.C. Leung, hep-lat/9711033; M.F.L. Golterman, Acta Phys. Polon. **B25** (1994) 1731.
- [29] P.H. Damgaard, hep-th/9711110; G. Akemann and P.H. Damgaard, hep-th/9802174; G. Akemann and P.H. Damgaard, hep-th/9801133.
- [30] K. Efetov, Adv. Phys. **32**, 53 (1983).
- [31] A.V. Andreev, B.D. Simons, and N. Taniguchi, Nucl. Phys **B432** [FS] (1994) 487.
- [32] J. Stern, hep-ph/9801282.
- [33] D.I. Diakonov and V.Yu. Petrov, Sov. Phys. JETP **62** (1985) 204.
- [34] D.I. Diakonov and V.Yu. Petrov, Nucl. Phys. **B 272** (1986) 457.
- [35] D.I. Diakonov and V.Yu. Petrov, Leningrad preprint LNPI-1153 (1986).
- [36] E.V. Shuryak and J.J.M. Verbaarschot, Nucl. Phys. **B410** (1993) 55.
- [37] T. Schäfer and E.V. Shuryak, hep-ph/9610451, Rev. Mod. Phys. (1998) (in press).
- [38] J. Verbaarschot and I. Zahed, Phys. Rev. Lett. **70**, 3852 (1993).
- [39] G. Akemann, P. Damgaard, U. Magnea and S. Nishigaki, Nucl. Phys. **B 487**[FS] (1997) 721.
- [40] E. Brézin, S. Hikami and A. Zee, Nucl. Phys. **B464** (1996) 411.
- [41] T. Guhr and T. Wettig, Nucl. Phys. **B506**, 589 (1997).

- [42] A.D. Jackson, M.K. Sener and J.J.M. Verbaarschot, Nucl. Phys. **B479**, 707 (1996); Nucl. Phys. **B506**, 612 (1997).
- [43] P.H. Damgaard, hep-th/9711047; P.H. Damgaard and S.M. Nishigaki, hep-th/9711023; S.M. Nishigaki, P.H. Damgaard and T. Wettig, hep-th/9803007; T. Wilke, T. Guhr and T. Wettig, hep-th/9711057; M.K. Sener and J.J.M. Verbaarschot, hep-th/9801042.
- [44] T. Guhr, private communication.
- [45] K. Jansen and C. Liu, Nucl. Phys. Proc. Suppl. **53** (1997) 974.
- [46] T. Schäfer and E.V. Shuryak, Phys. Rev. **D53** (1996) 6522.
- [47] S.J. Hands and M. Teper, Nucl. Phys. **B** (Proc. Suppl.) **42** (1995) 237.
- [48] A. Smilga and J. Stern, Phys. Lett. **B318** (1993) 531.
- [49] J.C. Osborn, D. Toublan and J.J.M. Verbaarschot, in preparation.
- [50] J.J.M. Verbaarschot, Acta Phys. Polon. **B25** (1994) 133.
- [51] C.M. Canali, M. Wallin and V.E. Kravtsov, cond-mat/9409123; Y. Chen and K.J. Eriksen, Int. J. Mod. Phys. B9 (1995) 1205.
- [52] M.A. Nowak, J.J.M. Verbaarschot and I. Zahed, Nucl. Phys. **B324** (1989) 1.
- [53] V.E. Kravtsov, in *Correlated Fermions and Transport in Mesoscopic Systems*, Les Arcs, 1996, cond/mat9603166.
- [54] F. Karsch and E. Laermann, Phys. Rev. **D50** (1994) 6954.